We are IntechOpen, the world's leading publisher of Open Access books Built by scientists, for scientists

4,800
Open access books available

122,000
International authors and editors

135M
Downloads

Our authors are among the

154
Countries delivered to

TOP 1%
most cited scientists

12.2%
Contributors from top 500 universities

CLARIVATE ANALYTICS BOOK CITATION INDEX INDEXED

WEB OF SCIENCE™

Selection of our books indexed in the Book Citation Index in Web of Science™ Core Collection (BKCI)

Interested in publishing with us?
Contact book.department@intechopen.com

Numbers displayed above are based on latest data collected.
For more information visit www.intechopen.com

11

Dead-Reckoning Method for Personal Navigation Systems Using Kalman Filtering Techniques to Augment Inertial/Magnetic Sensing

Angelo Maria Sabatini
ARTS Lab, Scuola Superiore Sant'Anna, Pisa, Italy

1. Introduction

Sensing techniques and computer algorithms help relieve demands in answering three questions that are crucial to navigation problem solving: "where am I?", "where am I going?", and "how should I get there?". The question "where am I?", namely localization, is addressed in this paper, in regard to the development of personal navigation systems (PNS) for determining a human walker's position and orientation. Biomedical applications of PNS technology, the ones we are mainly interested in, may include ambulatory monitoring systems for assessing the physical activity behavior of persons with disabilities and chronic health conditions, orientation & mobility aids for the blind or visually impaired, assistance services for frail seniors with compound problems of memory loss and disorientation.

In principle, PNS would provide the localization data in any environment, and at any time. Design criteria, in terms of, e.g., portability, accuracy, availability, cost, hindrance to the natural walking pattern, and the idiosyncrasies of the environment where the user walks greatly concur in practice to restrict the choice of sensing techniques and computational methods suited to implement PNS. Localization in outdoor environments is easy to solve using Global Positioning System (GPS) technology, despite that a number of serious shortcomings exist: loss of satellite track, when direct line of sight with the GPS constellation is precluded by obstructions, inability to provide static heading information, significant power consumption. When localization in indoor environments is pursued and GPS is therefore useless, other externally-referenced sensing techniques are available (video movement-sensing, infrared, ultrasound); however, their operation is typically based on complex and costly measuring hardware, dense environment infrastructure, not to mention the severely limited properties of the external sources themselves, in terms of, e.g., range, field-of-view and so forth.

Internally-referenced sensing techniques, namely inertial sensing, used in association with a relative-measurement approach, namely dead-reckoning (DR), can be a useful navigation alternative for implementing self-contained PNS (Fang et al., 2005). Being internally referenced and immune to interference and shadowing, inertial sensors (accelerometers and gyros) sense movement, in principle, without restrictions in the spatial domain (Welch &

Source: Kalman Filter: Recent Advances and Applications, Book edited by: Victor M. Moreno and Alberto Pigazo,
ISBN 978-953-307-000-1, pp. 584, April 2009, I-Tech, Vienna, Austria

Foxlin, 2002). The main problem of a dead-reckoning approach to localization based on inertial sensing is represented by the need to time-integrate the inertial measurements, which include any superimposed sensor drift and noise. Hence, the localization errors tend to grow unbounded over time, with the position errors growing at a faster rate than the orientation errors (Foxlin, 2002). Another drawback is that the integration has to be started from initial conditions, which inertial sensors cannot help establishing, or disambiguating completely. Earth's magnetic field sensing – an externally-referenced sensing technique whose source is virtually available anywhere on the Earth's surface – can help mitigate the integration errors and specify the absolute orientation. Inertial and magnetic sensors are thus an interesting sensor suite for PNS; recent technological advances have enabled fully integrated inertial/magnetic measurement units (IMMU) with form factors, cost and metrological specifications suited to studies in the field of human movement (Yun & Bachmann, 2006).

In this chapter we present a shoe-mounted inertial/magnetic sensor system to estimate the three-dimensional (3D) path traveled by the foot instep of an ambulating person. Central to our approach are the computer algorithms which estimate the IMMU orientation in the 3D space via a quaternion-based adaptive Extended Kalman Filtering (EKF), and determine the traveled path by stride-wise strap-down double integration of foot accelerations resolved in the navigation frame. In order to make the filtering process robust against the disturbances which may affect the IMMU sensors , several tricks are incorporated in the developed EKF:

- adaptation of the measurement noise covariance matrix during EKF runs;
- adaptive alternation between initialization and run of the EKF, so as to refine the estimation of either the rotation quaternion or the magnetic sensor bias vector – this is based on stance/swing phase gait detection driven by gyroscopic data, and accelerometric/magnetic measurement validation;
- bias-correction of the magnetic sensor measurements before using them for initializing each EKF run;
- stride-wise integration of gravity-compensated acceleration components with zero velocity updates performed once every movement epoch is detected.

2. Related work

Most PNS pursue the following approach to locate the position of the user: the displacement from the previous known position is computed from the step length of the user and his heading. Suppose a sensor, e.g., an accelerometer, is used to detect a step (many PNS are waist-mounted, in the belief that the dynamics of human movements is less challenging in those body parts where amplitude range and frequency content of sensed accelerations are limited). The vertical acceleration measured by a waist-mounted accelerometer takes its maximal absolute value when each foot hits the ground. The step time can thus be estimated by peak detection algorithms. The step length is usually either predetermined and entered by the user as a calibration factor (electronic pedometer), or estimated on the basis of simple biomechanical models. Provided that the step length is multiplied by the number of detected steps, the traveled distance is then computed.

In (Ladetto & Merminod, 2002), a walking model is used to predict the relationship between step time and step length in normal walking patterns. Similarly, the existence of simple relationships between step time, RMS value of the norm of the waist acceleration, and step

length during normal walking is exploited in (Perrin et al., 2000). The main difficulties with the model-based approach to step length estimation are: the need for individual adaptations to, e.g., the walked surface (uphill/level/downhill walking) and its nature; the difficulty to encompass the large variety of motor patterns that, especially in crowded environments, a human walker produces to functionally move his body. As for the former point, additional sensor systems have to be deployed for in-line parametric model calibration, e.g., GPS and altimeters; as for the latter point, pattern recognition algorithms have to be implemented to discriminate walking from non-walking activities, e.g., side-stepping. Most PNS use a magnetic compass as a heading sensor (Ladetto & Merminod, 2002; Lee & Maze, 2002; Jirawimut et al., 2003). The accelerometers are used in these systems to perform the important task of tilt compensation, so as to project the measured Earth's magnetic field vector in the horizontal plane. However, since the Earth's magnetic field is weak and it can be easily masked and unpredictably distorted by any sort of natural or man-made magnetic disturbance, computational intelligence is mandatory in the design of complementary filtering algorithms which help improve the accuracy of compass heading determination using additional sensors, e.g., gyros, GPS or both.

An alternative approach to locate the position of the user is by strap-down integration (Elwell, 1999). The problems with this approach are due to the tendency of DR errors to grow over time – either errors incurred in estimating the absolute orientation of the navigation sensor, or errors incurred in performing the double-integration of gravity-compensated linear accelerations. In spite that the human body dynamics is more challenging at the foot level than it is at the waist level, the foot is a convenient location for PNS mounting when the goal is to measure directly the traveled distance (Sabatini et al., 2005). In particular, we may take advantage of the fact that the foot is stationary during the stance phase of gait. When the PNS is stationary, zero velocity updates (velocity errors can be reset with each stride), and zero attitude updates (gyro bias drift can be estimated and subtracted from gyro sensor output) can be performed. The benefits of these procedures are examined in (Sabatini, 2005), which highlights the importance that strap-down integration of inertial measurements is performed in a stride-wise fashion. When the foot is stationary, gravimetric tilt sensing, alone or combined with compass heading determination, helps establish the initial conditions needed to carry out another round of strap-down integration during the next gait cycle.

In (Sabatini et al., 2005), a sensor unit, which is composed of one uni-axis gyro, oriented in the medio-lateral direction, and one bi-axis accelerometer, with sensitive axes embedded in the vertical plane, is fastened to the foot instep in order to estimate a number of spatio-temporal features of gait, including walked distance, average walking speed, incline of the walked surface, stride length, stride time, and relative stance. The angular velocity measured by the gyro is used to perform gait segmentation in different phases, including the phase when the sensor unit alignment is performed by gravimetric tilt sensing. Treadmill walking trials attest the good accuracy of the proposed approach. The main limitation is that the system is blind to changes in the direction of displacement. These limitations can be overcome, in principle, when a fully integrated IMMU is considered, as it is in (Veltink et al., 2003) where, although experimental waveforms of the foot Euler angles are reported, no experimental results are offered in terms of user localization. Another interesting solution is described in (Stirling et., 2005), where the sensing hardware includes a pair of dual-axis accelerometers, with sensitive axes that are either collinear (X-axis) or

parallel (Y-axis), and a dual-axis magnetic sensor. The accelerometers are offset to allow angular acceleration measurement. Since the sensor orientation is computed from a stride-wise double-integration of acceleration data, however, the overall accuracy of the system may be less than the accuracy achievable with a more expensive gyro-based IMMU.

3. Method

3.1 The strap-down approach to inertial navigation

Suppose a coordinate system attached to a rigid body in space – the body frame B, and an Earth's reference frame E are introduced. For the orientation and position of the rigid body to be determined, the orientation of the axes of B with respect to the E, and the origin of B relative to E need to be specified. Be $\vec{\mathbf{x}}$ a 3×1 column-vector, which is resolved along the axes of B and E, to yield $\vec{\mathbf{x}}^B$ and $\vec{\mathbf{x}}^E$, respectively:

$$\vec{\mathbf{x}}^B = \overset{E\to B}{C}\,\vec{\mathbf{x}}^E \tag{1}$$

where $\overset{E\to B}{C}$ is the direction cosine matrix (DCM) for the transformation from E to B.

Directly or through using attitude parameterizations based on, e.g., the orientation vector or the rotation quaternion, the DCM can be numerically determined by integrating a system of first-order differential equations that involve the components of the instantaneous angular velocity vector $\vec{\boldsymbol{\omega}}^B = [p, q, r]^T$, which can be measured by a tri-axis gyro strapped to the rigid body (Sabatini, 2006); the initial conditions needed to integrate these equations are assumed to be known or measurable during the alignment process. Alternately, the DCM can be determined by vector matching in E and B (Shuster and Oh, 1981). Vector matching, also known as Wahba's problem, matches two non-collinear vectors that are known in E and are measured in B – the Earth's gravity field $\vec{\mathbf{g}}^E = [0,0,g]^T$ (g = 9.81 m/s² is the gravity acceleration) and the Earth's magnetic field $\vec{\mathbf{h}}^E = [h_x,0,h_z]^T$, both normalized to have unit norm, are two these *reference* vectors; aiding sensors, such as a tri-axis accelerometer and a tri-axis magnetic sensor, can thus be strapped to the rigid body, in order to resolve, respectively, the Earth's gravity and magnetic fields as unit-norm *observation* vectors in B. Vector matching may help solve the alignment process and is, in principle, an alternative to using gyros for DCM determination when the body accelerations, due to its own movement, are negligible in comparison with gravity (Gebre-Egziabher et al., 2000).

The estimated DCM is used to perform the process of gravity-compensation in the accelerometer output signals:

$$\vec{\mathbf{a}}_o^E(t) = \overset{B\to E}{C}(t)\,\vec{\mathbf{a}}^B(t) - \vec{\mathbf{g}}^E \tag{2}$$

Finally, the velocity $\vec{\mathbf{v}}_o{}^E(t)$ and position of the rigid body $\vec{\mathbf{p}}_o{}^E(t)$ are determined by single and double integration of (2), respectively.

The strap-down approach to inertial navigation as summarized above is deceptively simple. The computations of the integrals that are involved in determining the orientation from measured angular velocities, and determining the linear velocity/displacement from gravity-compensated accelerations are susceptible to several error sources, including the sensors' bias offset, drift, calibration errors, and the random-walk errors associated with

wideband noise integration. Also, the influence of body movements and external magnetic disturbances on the accuracy of accelerometers and magnetic sensors to sense the reference Earth's gravity and magnetic fields greatly contribute to the overall error budget.
It is then difficult that high performance in orientation/position determination are achieved by relying on IMMU sensors, the stand-alone accuracy and run-to-run stability of which are poor. In literature, the commonest approaches to enhance the achievable navigation performance consist of integrating additional sensorial resources, e.g., GPS into the navigation system hardware, managing the sensor fusion via sophisticated Kalman filters running in the navigation system software, or both (Foxlin, 2002; Ladetto & Merminod, 2002). Our approach is to use unaided inertial/magnetic sensing, in combination with an EKF for orientation determination. The structure of the developed EKF and the tricks introduced to enhance the filter performance are described in the next Section.

3.2 Implementation

The flow of information underlying the strap-down approach to inertial navigation we propose for the shoe-mounted IMMU described in this paper is sketched in Fig. 1.

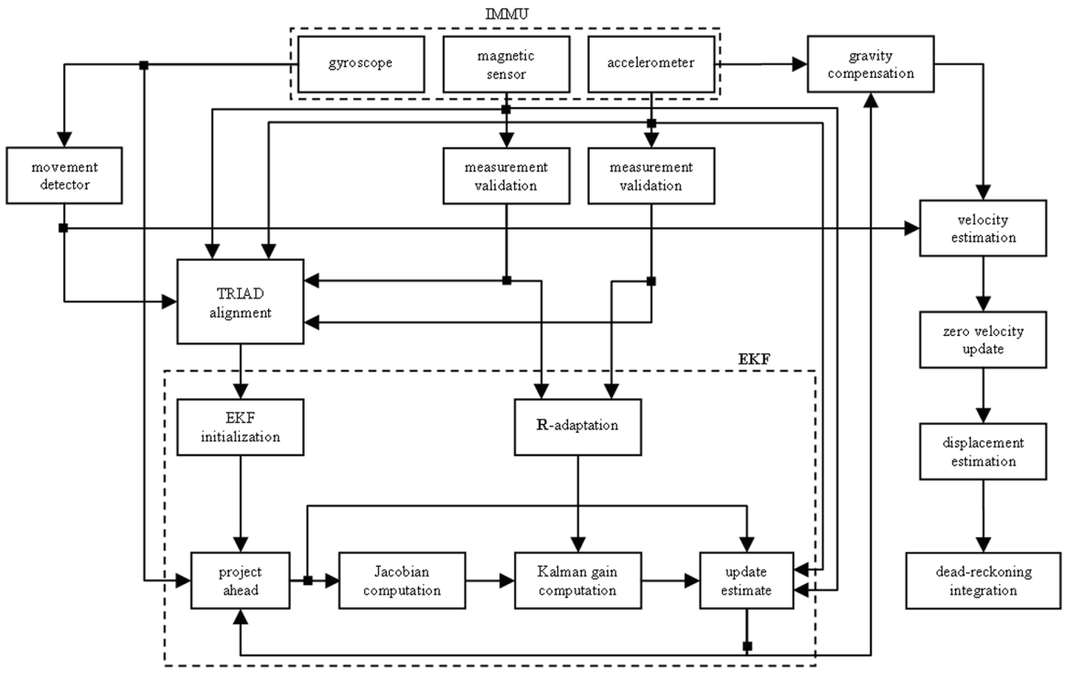

Fig. 1. Information flow for the proposed dead-reckoning algorithm of personal navigation.

The attitude parameterization we choose is the quaternion $\mathbf{q} = [\vec{\mathbf{e}}^T, q_4]^T$ associated to the rotation from B to E ($\vec{\mathbf{e}} = [q_1, q_2, q_3]^T$ is the vector part and q_4 is the scalar part of the quaternion). The rigid body angular movement obeys the vector differential equation

$$\frac{d}{dt}\mathbf{q} = \mathbf{\Omega}\left[\vec{\boldsymbol{\omega}}^B\right]\mathbf{q} = \begin{bmatrix} 0 & -r & q & p \\ r & 0 & -p & q \\ -q & p & 0 & r \\ p & q & r & 0 \end{bmatrix}\mathbf{q} \tag{3}$$

whose discrete-time model is

$$\begin{cases} \mathbf{q}_{k+1} = \exp(\mathbf{\Omega}_k T_s)\,\mathbf{q}_k, \quad k = 0,1,... \\ \mathbf{q}_0 = \mathbf{q}(0), \end{cases} \tag{4}$$

where T_s is the system's sampling interval. The quaternion is determined at time instants kT_s, starting from initial conditions $\mathbf{q}_0$ obtained in the alignment process. For (4) to be valid, the angular velocity $\vec{\boldsymbol{\omega}}_k$ is to be approximately constant in the interval $[kT_s, (k+1)T_s]$. The DCM is a homogeneous quadratic function of the components of $\mathbf{q}$:

$$\overset{E\to B}{C}(\mathbf{q}) = \left(q_0^2 - \left\|\vec{\mathbf{e}}\right\|^2\right)\mathbf{I}_{3\times 3} - 2q_4 \begin{bmatrix} 0 & -q_3 & q_2 \\ q_3 & 0 & -q_1 \\ -q_2 & q_1 & 0 \end{bmatrix} + 2\vec{\mathbf{e}}\,\vec{\mathbf{e}}^{\,T} \tag{5}$$

which is used for updating the DCM, once that the solution of (4) has progressed in time.
In this paper the alignment process is performed using the TRIAD algorithm (Shuster & Oh, 1981). Given two *reference* unit vectors, namely $\vec{\mathbf{v}}_1$ and $\vec{\mathbf{v}}_2$, and two *observation* unit vectors, namely $\vec{\mathbf{w}}_1$ and $\vec{\mathbf{w}}_2$, the DCM is estimated by the TRIAD algorithm as follows:

$$\overset{E\to B}{C}_{est} = \left[\vec{\mathbf{s}}_1 \quad \vec{\mathbf{s}}_2 \quad \vec{\mathbf{s}}_3\right]\left[\vec{\mathbf{r}}_1 \quad \vec{\mathbf{r}}_2 \quad \vec{\mathbf{r}}_3\right]^T \tag{6}$$

where:

$$\begin{aligned} \vec{\mathbf{r}}_1 &= \vec{\mathbf{v}}_1 \\ \vec{\mathbf{r}}_2 &= \vec{\mathbf{v}}_1 \times \vec{\mathbf{v}}_2 \\ \vec{\mathbf{r}}_3 &= \vec{\mathbf{r}}_1 \times \vec{\mathbf{r}}_2 \end{aligned} \tag{7}$$

and:

$$\begin{aligned} \vec{\mathbf{s}}_1 &= \vec{\mathbf{w}}_1 \\ \vec{\mathbf{s}}_2 &= \vec{\mathbf{w}}_1 \times \vec{\mathbf{w}}_2 \\ \vec{\mathbf{s}}_3 &= \vec{\mathbf{s}}_1 \times \vec{\mathbf{s}}_2 \end{aligned} \tag{8}$$

where × denotes the cross vector product. Suppose that the accelerometer and magnetic sensor measurement noises are modeled as Gaussian white noises, with null mean and covariance matrices $\Sigma_a = \sigma_a^2\mathbf{I}$ and $\Sigma_h = \sigma_h^2\mathbf{I}$, respectively ($\mathbf{I}$ is the 3×3 identity matrix). The covariance matrix of the TRIAD-related quaternion is known to be a function of the observation vectors and sensor noise variances (Shuster & Oh, 1981):

$$P^{TRIAD} = f\left(\vec{\mathbf{w}}_1, \vec{\mathbf{w}}_2, \sigma_1^2, \sigma_2^2\right) \tag{9}$$

where $\sigma_1^2 = \sigma_a^2, \sigma_2^2 = \sigma_h^2$ or $\sigma_1^2 = \sigma_h^2, \sigma_2^2 = \sigma_a^2$; it can be used for EKF initialization at first contact.
The minute body movements at the time of alignment acts to increase σ_a over the noise floor that is measured when the tri-axis accelerometer stands motionless on the calibration bench. More importantly, the accuracy of the TRIAD-quaternion is actually dependent on

whether systematic errors affect the observation vectors, which invalidates the assumption that the sensor measurements are unbiased. Suppose, indeed, that the tri-axis magnetic sensor output is expressed by

$$\vec{\mathbf{m}} = {}^{m}\mathbf{K}\,{}^{E\to B}_{\;\;\;\;}\mathbf{C}(\mathbf{q})\,\vec{\mathbf{h}}^{E} + {}^{h}\vec{\mathbf{b}} + {}^{h}\vec{\mathbf{v}} \tag{10}$$

where ${}^{m}\mathbf{K}$ is the scale factor matrix (ideally, ${}^{m}\mathbf{K} = \mathbf{I}$); ${}^{h}\vec{\mathbf{b}}$ is the bias vector (ideally, it is null); ${}^{h}\vec{\mathbf{v}}$ is the zero-mean magnetic sensor measurement noise. Even though it is carefully calibrated against the effects of sensor electronic offset and scale factor drifts, and the effects of so-called hard and soft irons due to sensor placement on the human body, the tri-axis magnetic sensor is vulnerable to either static or time-varying external magnetic disturbances near or within the measurement space (Sabatini, 2006). The following discrete-time random-walk model is used to describe the dynamics of the (time-varying) bias vector:

$${}^{h}\vec{\mathbf{b}}_{k+1} = {}^{h}\vec{\mathbf{b}}_{k} + {}^{h}\vec{\mathbf{w}}_{k} \tag{11}$$

where ${}^{h}\vec{\mathbf{w}}_{k}$ is a zero-mean white noise process with covariance matrix ${}^{m}\mathbf{\Sigma} = \sigma_{w}^{2}\,\mathbf{I}$.
The state vector of the developed EKF includes the rotation quaternion and the magnetic bias vector. The state transition vector equation is

$$\vec{\mathbf{x}}_{k+1} = \begin{bmatrix} \mathbf{q}_{k+1} \\ {}^{h}\vec{\mathbf{b}}_{k+1} \end{bmatrix} = \Phi(T_s, \vec{\boldsymbol{\omega}}_k)\,\vec{\mathbf{x}}_k + \vec{\mathbf{w}}_k = \begin{bmatrix} \exp(\mathbf{\Omega}_k T_s) & \mathbf{0} \\ \mathbf{0} & \mathbf{I} \end{bmatrix} \begin{bmatrix} \mathbf{q}_k \\ {}^{h}\vec{\mathbf{b}}_k \end{bmatrix} + \begin{bmatrix} {}^{q}\vec{\mathbf{w}}_k \\ {}^{h}\vec{\mathbf{w}}_k \end{bmatrix} \tag{12}$$

where $\mathbf{0}$ is the 3×3 null matrix and

$${}^{q}\vec{\mathbf{w}}_k = -\frac{T_s}{2}\mathbf{\Xi}_k\,{}^{g}\vec{\mathbf{v}}_k = -\frac{T_s}{2}\begin{bmatrix} [\vec{\mathbf{e}}_k \times] + q_{0k}\mathbf{I} \\ -\vec{\mathbf{e}}_k^{T} \end{bmatrix} {}^{g}\vec{\mathbf{v}}_k \tag{13}$$

where the operator

$$[\vec{\mathbf{e}}_k \times] = \begin{bmatrix} 0 & -e_z & e_y \\ e_z & 0 & -e_x \\ -e_y & e_x & 0 \end{bmatrix} \tag{14}$$

represents the cross vector product.
${}^{g}\vec{\mathbf{v}}_k$ is the gyro measurement noise, assumed to be a zero-mean white Gaussian process, with covariance matrix ${}^{g}\mathbf{\Sigma}_k = \sigma_g^2\mathbf{I}$. The process noise covariance matrix $\mathbf{Q}_k$ has the following expression:

$$\mathbf{Q}_k = \begin{bmatrix} (T_s/2)^2\,\mathbf{\Xi}_k\mathbf{\Sigma}_g\mathbf{\Xi}_k^{T} & \mathbf{0} \\ \mathbf{0} & {}^{m}\mathbf{\Sigma}_k \end{bmatrix} \tag{15}$$

The measurement model is given by

$$\vec{\mathbf{z}}_{k+1} = \begin{bmatrix} {}^{h}\vec{\mathbf{m}}_{k+1} \\ {}^{a}\vec{\mathbf{m}}_{k+1} \end{bmatrix} = \mathbf{f}\left[\vec{\mathbf{x}}_{k+1}\right] + \vec{\mathbf{v}}_{k+1} = \begin{bmatrix} {}^{E\to B}_{\;\;\;\;}\mathbf{C}(\mathbf{q}_{k+1})\,\vec{\mathbf{h}}^{E} \\ {}^{E\to B}_{\;\;\;\;}\mathbf{C}(\mathbf{q}_{k+1})\,\vec{\mathbf{g}}^{E} \end{bmatrix} + \begin{bmatrix} {}^{h}\vec{\mathbf{b}}_{k+1} \\ \mathbf{0} \end{bmatrix} + \begin{bmatrix} {}^{h}\vec{\mathbf{v}}_{k+1} \\ {}^{a}\vec{\mathbf{v}}_{k+1} \end{bmatrix} \tag{16}$$

The covariance matrix of the measurement model $\mathbf{R}_{k+1}$ is

$$\mathbf{R}_{k+1} = \begin{bmatrix} {}^{h}\mathbf{R}_{k+1} & \mathbf{0} \\ \mathbf{0} & {}^{a}\mathbf{R}_{k+1} \end{bmatrix} \tag{17}$$

Underlying (17) is the assumption that the magnetic sensor and accelerometer measurement noise ${}^{h}\vec{\mathbf{v}}_{k+1}$ and ${}^{a}\vec{\mathbf{v}}_{k+1}$ are uncorrelated zero-mean white noise processes, the covariance matrices of which are ${}^{h}\mathbf{R}_{k+1}={}^{R}\sigma_{h}^{2}\mathbf{I}$ and ${}^{a}\mathbf{R}_{k+1}={}^{R}\sigma_{a}^{2}\mathbf{I}$, respectively.
Before the current measurement $\vec{\mathbf{z}}_{k+1}$ is incorporated in the filtering process to drive the state vector update, a mechanism of adaptation of the measurement noise covariance matrix is implemented. In our approach, the deviation of the sensed magnetic field magnitude from the local earth's magnetic field magnitude is tested and the following adaptation mechanism is then implemented:

$${}^{R}\sigma_{h}^{2} = \begin{cases} \sigma_{ho}^{2}\left| \dfrac{\left\| \vec{\mathbf{m}}_{k+1} \right\|}{\left\| \vec{\mathbf{h}} \right\|} - 1 \right|, & \left| \left\| \vec{\mathbf{m}}_{k+1} \right\| - \left\| \vec{\mathbf{h}} \right\| \right| < \varepsilon_{m} \\ \infty \text{ (measurement rejected)}, & \text{otherwise} \end{cases} \tag{18}$$

Moreover, the measured acceleration magnitude is tested in advance for the absence of significant deviations from gravity; if persistent for some specified time interval, this absence is considered the sign that the body is at rest. If not so, the observation variance ${}^{R}\sigma_{a}^{2}$ is set to extremely high values:

$${}^{R}\sigma_{a}^{2} = \begin{cases} \sigma_{a}^{2}, & \left| \left\| \vec{\mathbf{a}}_{j+1} \right\| - \left\| \vec{\mathbf{g}} \right\| \right| < \varepsilon_{a} \quad \forall j \in [k-k_{a}, k] \\ \infty \text{ (measurement rejected)}, & \text{otherwise} \end{cases} \tag{19}$$

Because of the non-linear nature of the measurement model (16), the EKF approach requires that a first-order Taylor-Mac Laurin expansion is carried out around the current state estimate by computing the Jacobian matrix:

$$\mathbf{F}_{k+1} = \frac{\partial}{\partial \vec{\mathbf{x}}_{k+1}} \vec{\mathbf{z}}_{k+1} \Big|_{\vec{\mathbf{x}}_{k+1}=\vec{\mathbf{x}}_{k+1}^{-}} \tag{20}$$

For the sake of reader's convenience, the EKF equations are summarized below. We remind that the superscript – in the following equations stands for *a priori* estimate at time t_{k+1}, before the current measurement $\vec{\mathbf{z}}_{k+1}$ is used in the computation of the *a posteriori* estimate.

- Compute the *a priori* state estimate:

$$\vec{\mathbf{x}}_{k+1}^{-} = \Phi(T_s, \vec{\boldsymbol{\omega}}_k)\vec{\mathbf{x}}_k$$

- Compute the *a priori* error covariance matrix

$$\mathbf{P}_{k+1}^{-} = \Phi(T_s, \vec{\boldsymbol{\omega}}_k)\mathbf{P}_k\Phi(T_s, \vec{\boldsymbol{\omega}}_k)^T + \mathbf{Q}_k$$

- Compute the Kalman gain

$$\mathbf{K}_{k+1} = \mathbf{P}_{k+1}^{-}\mathbf{F}_{k+1}^{T}\left(\mathbf{F}_{k+1}\mathbf{P}_{k+1}^{-}\mathbf{F}_{k+1}^{T} + \mathbf{R}_{k+1}\right)^{-1}$$

- Compute the *a posteriori* state estimate

$$\vec{\mathbf{x}}_{k+1} = \vec{\mathbf{x}}_{k+1}^{-} + \mathbf{K}_{k+1}\left[\vec{\mathbf{z}}_{k+1} - \mathbf{f}\left(\vec{\mathbf{x}}_{k+1}^{-}\right)\right]$$

- Compute the *a posteriori* error covariance matrix

$$\mathbf{P}_{k+1} = \mathbf{P}_{k+1}^{-} - \mathbf{K}_{k+1}\mathbf{F}_{k+1}\mathbf{P}_{k+1}^{-}$$

Although similar in principle, the developed EKF is different in several regards from the EKF described in (Sabatini, 2006). First, the accelerometer bias vector is not part of the state vector; second, the test (18) does not include the condition on the dip angle, namely the angle between the sensed gravity and magnetic fields; third, the magnetic sensor variance in (18) is made to increase over σ_{ho}^2 based on the magnitude of sub-threshold magnetic disturbances.

More importantly, a central role in the EKF operation is now played by the action of the movement detector, Fig. 1. The gyro output signal feeds the movement detector, the function of which is to discriminate conditions of presence and absence of movement by submitting the norm of the measured angular velocity vector to a threshold-based detector. The movement detector helps identify, in each gait cycle, the time interval between heel-off and foot-flat, when the foot instep swings and gyro data can be exploited by the EKF to update the estimate of the state vector. Conversely, when the foot instep is detected to be steady at 0 °/s, the EKF does not run and its initialization at first contact is performed by applying the TRIAD algorithm to the aiding sensors' information available before the heel-off transition, in preparation for the next gait cycle.

It is the outcome of the measurement validation tests (18)-(19) which drives the alternation between EKF initializations during stance and EKF runs during swings. If the test (19) fails at the time when the movement detector signals the transition from absence to presence of movement, the EKF initialization is not actually carried out, and the EKF processing is extended to the following gait cycle. Conversely, upon successful termination of the test (19), it is the outcome of the test (18) to prescribe whether body-fixed magnetic sensor measurements are subject to bias compensation before applying the TRIAD algorithm. Whilst no bias compensation takes place when the test (18) is successfully terminated, the estimate of the bias vector delivered by the EKF at the time when the test (18) fails is used for compensation purposes in what we call the iterated-TRIAD algorithm. The movement detector may be unable to cope with small changes of orientation when non-walking activities, e.g., foot shuffling during rest periods, are chained with epochs of normal walking; hence, the EKF-estimated bias vector has to be resolved in *B* without knowing the rotation quaternion, which is, indeed, the quantity that the TRIAD algorithm would determine using quasi-static acceleration and bias-corrected magnetic field measurements. The estimate of the state vector delivered by the EKF at the time when the test (18) fails helps correct body-fixed magnetic sensor measurements before applying the TRIAD algorithm. The quaternion determined by the TRIAD algorithm is then used to refine the estimate of the bias vector in *B*, before applying the TRIAD algorithm again. The interplay

between applications of the TRIAD algorithm and refinements of the bias vector estimate resolved in B proceeds iteratively, until convergence is reached – this occurs either when the difference between rotation quaternions determined in successive iterations is smaller than a given threshold, or when a maximum number of iterations is elapsed.
The gravity compensation of acceleration components is performed using the rotation quaternion estimated from the EKF. In order to maximally benefit from the zero velocity update, the velocity estimate is reset with each time interval between heel-off and foot flat (determined by the movement detector), before embarking in the second integration which helps update the position of the foot instep relative to E from its most recent position fix.

3.3 Experimental validation

The dead-reckoning navigation algorithm was tested in a series of walking trials with data acquired from a shoe-mounted IMMU, Fig. 2.
A MicroStrain 3DM-GX1 sensor device embedded with a tri-axis gyro, accelerometer, and magnetic sensor (MicroStrain Inc., Williston, VT, U.S.A.) was placed on the instep of the (left) foot and attached snugly to the shoe under the shoe-laces. The device was interfaced to a PC via a serial communication interface (RS232 communication protocol, baud rate: 115.200 bps). The raw sensory data were delivered at a sampling rate of about 77 Hz, and submitted to off-line processing using Matlab v. 6.0. After the raw data were filtered with a second-order forward-backward low-pass Butterworth filter (cut-off frequency: 10 Hz), the rotation quaternion was determined by directly time-propagating (4) over the whole data-set. Zero velocity updates applied to gravity-compensated acceleration components and successive integration of detrended velocity components enabled to produce the displacements of the foot instep from the start position.

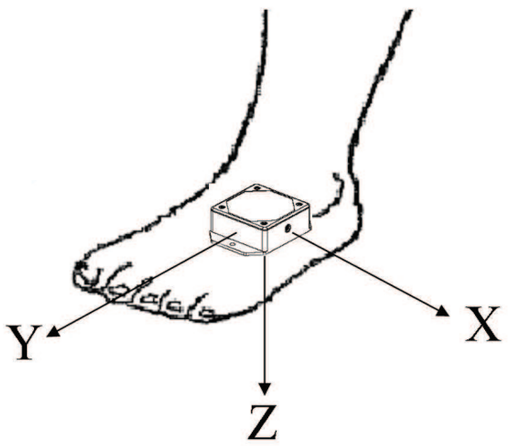

Fig. 2. Shoe-mounted IMMU, with the body-fixed reference frame superimposed.

Two EKF implementations were considered, henceforth called Method A and Method B. The difference between them was that the alternation between EKF initializations during stance and EKF runs during swings was adaptive, since it was based on the outcome of the measurement validation tests (18)-(19), and required to perform bias compensation of body-fixed magnetic sensor measurements, as prescribed by the TRIAD algorithm (Method A); conversely, the alternation was not adaptive and the TRIAD algorithm was applied without bias compensation in Method B.

The experimental validation consisted of walking along an outdoor path whose length was about 680 m, with overall changes in altitude of about 40 m. The path was walked in about 13 min. The instructions to the user were to walk in a stop-and-go fashion: walk ten consecutive strides before taking a brief rest, then walk ten consecutive strides, and so forth. The walker was also asked to turn around on himself at some point along the path, and the path traveled so far was then traced back. The truth-reference trajectory was constructed using a handheld GPS receiver (eMap, Garmin International Inc., Olathe, Kansas, U.S.A.), which was manually commanded by the user to store a way-point any time he rested between successive blocks of ten strides. In the open environment where the experiment was performed, the number of satellites in view was always between 5 and 7, hence the GPS receiver worked in nearly optimal conditions.

The EKF parameters were hand-crafted carefully by standard trial-and-error procedures. In our testing environment, a good parameter setting was the following: $\sigma_g = 0.6$ °/s, $\sigma_w = 1$ mGauss, $\sigma_{ho} = 1$ mGauss, $\sigma_a = 10$ mg. Additionally, as for the measurement validation tests (18)-(19), we choose $\varepsilon_m = 10$ mGauss, $\varepsilon_a = 0.1$ m/s^2, and $k_a T_s = 0.1$ s.

The filtering performance metrics was based on the root mean square (RMS) of the horizontal and vertical positioning error Δp_h and Δp_v, respectively, which were computed, together with the three-dimensional positioning error Δp.

4. Results

The time functions of the angular velocity (vector norm and X-axis component) sensed by the tri-axis gyro in two movement epochs occurring during the outdoor walking trial are reported in Fig. 3. The two movement epochs correspond to a representative downhill gait cycle, and to the user's turn-around maneuver.

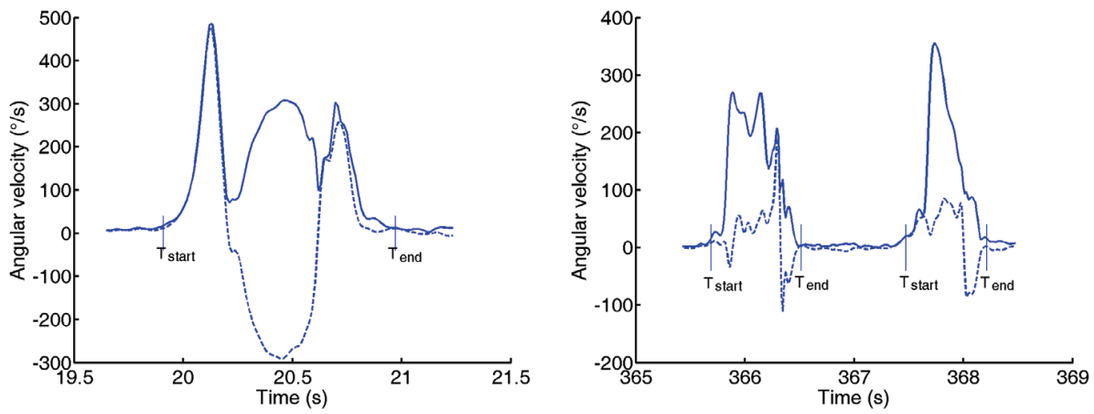

Fig. 3. Time function of the angular velocity sensed by the tri-axis gyro.
Solid line: vector norm; dashed line: X-axis component.
(a): representative gait cycle;
(b): movement patterns acquired during the turning around maneuver, see text.

The vector norms of the acceleration and magnetic field sensed by the aiding sensors are plotted against the times of alignment at which they are measured in Figs. 4-5.

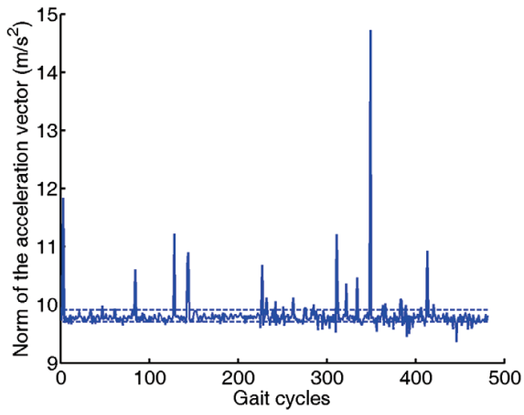

Fig. 4. Vector norm of the acceleration sensed by the tri-axis accelerometer at the time of alignment, as a function of the number of gait cycles.

The number of rejections issued by the measurement validation tests, normalized to the 481 movement epochs detected by the movement detector, are 7%, 21% and 1.25% (h-rejections, g-rejections and h/g-rejections). The EKF runs may thus have different durations: in particular, for Method A, the duration of each run depends whether (19) accepts the gravity read-out from the accelerometer at start and end times, which leads to the time function plotted in Fig. 6.

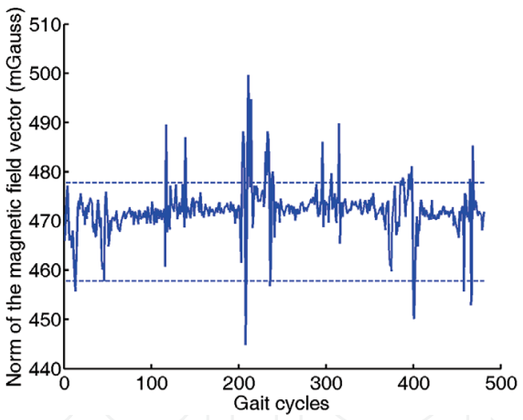

Fig. 5. Vector norm of the magnetic field sensed by the tri-axis magnetic sensor at the time of alignment, as a function of the number of gait cycles.

Conversely, the duration of each strap-down double integration of the gravity-compensated linear acceleration vector is related, for either Method A or B, to the duration of the corresponding movement epoch, see Fig. 7. Table 1 reports the RMS values of Δp achieved by Method A and B (about 0.6% of the total walked distance). If the EKF is run continuously, the positioning errors sum up to 129 m (horizontal) and 2 m (vertical). The DR trajectory, projected in the horizontal plane of the Earth's reference frame, is reported in Fig. 8, with the coordinates of the GPS way-points superimposed to it.

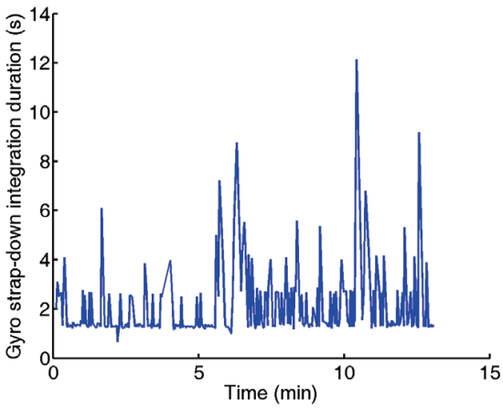

Fig. 6. Time duration of each EKF run, as a function of the time from start.

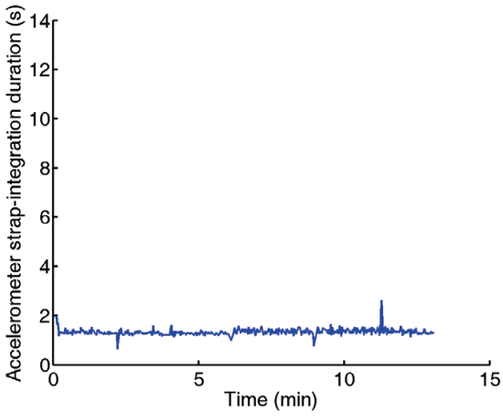

Fig. 7. Time duration of each gait cycle, as a function of the time from start.

	Δp_h [m]	Δp_v [m]	Δp [m]
A	2.1	3.6	4.1
B	2.4	3.7	4.4

Table 1. Values of horizontal, vertical, total positioning errors incurred by Method A and B.

The mean ± SD of the Euler angles of the foot (roll and pitch), measured at the time of alignment from the rotation quaternion delivered by the EKF (Method A), are reported in Table 2.

	uphill	downhill
roll angle [°]	21.6 ± 2.1	36.7 ± 1.5
pitch angle [°]	-16.2 ± 3.3	-5.9 ± 2.5

Table 2. Values of mean and standard deviation of the roll, pitch Euler angles measured at the time of alignment with Method A.

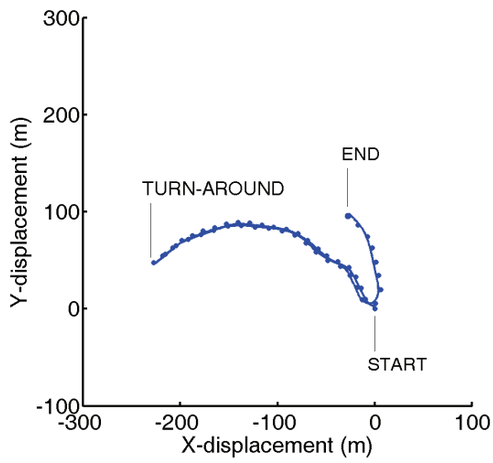

Fig. 8. Dead-reckoning trajectory reconstructed by the IMMU, and superimposed way-points collected from the GPS unit.

The statistics are averaged over the downhill and the uphill portions of the path, separately. Based on these data, the incline of the walking surface (in the direction of travel) turns out to be, on average, 7.5° (relative to the horizontal plane in the Earth's reference frame). The incline, estimated from the horizontal and vertical components of the DR trajectory, turns out to be 7.6° and 7.3° (downhill and uphill portions of the path, respectively).

5. Discussion and conclusions

Both methods A and B behave exactly in the same way when g-rejections do not occur: the procedure of alternation between TRIAD-based EKF initializations and EKF runs in both methods is, indeed, identical, since the movement detection module works for both methods on the same noisy angular velocity vector. However, in the interplay between initialization and run of the EKF, and in the face of the difficulty of performing double integration of gravity-compensated linear accelerations, the movement detector plays a very important role. It is the movement detector which identifies movement epochs based on signal thresholding. In our previous work, we have verified that movement detection is better handled by feeding gyro output signals, rather than acceleration output signals, to a movement detector. In (Sabatini et al., 2005) the signal from a gyro oriented in the user's medio-lateral direction is used for detecting a number of gait events, including heel-strike and toe-off. In order to detect movement epochs based on non-walking patterns, we propose to use here the norm of the angular velocity vector. Figs. 3-4 shows the difference between using the norm or a single component of the angular velocity vector, i.e., the X-axis component, which is approximately in the user's medio-lateral direction. While, for a representative gait cycle, the difference is minimal, the movement detector introduces a small delay when the turn-around maneuver is analyzed via the X-axis gyro output signal.

In the configuration of shoe-mounted IMMU studied in this paper, the threshold setting is not overly difficult, unless the walking speed increases too much, such that time intervals when the body part (the foot instep, here) is steady are critical to identify. In this regard, however, it should be pointed out that the accurate tracking of foot movements involved in fast walking, jogging or running is, above all, undermined by limitations in the gyro maximum sensing range. When the thresholds are too low, gyro measurement noise may erroneously lead to identify movement epochs when they do not exist; however, provided that the duration of these movement artifacts is not excessive, their effect on the overall positioning/orientation accuracy is generally quite limited. Due to an inadequately low threshold setting, the motion detector may be missing the end of a movement epoch, with the consequence of delaying the time of the zero velocity update; conversely, when the thresholds are too high, either the start of a movement epoch is delayed, or its end is anticipated, so that a moving body part is misleadingly considered motionless; the consequences are that the EKF initialization step and the zero velocity update are applied at the wrong time. The threshold setting used in this paper is hand-crafted to work properly on the outdoor walking trial data-set.

The DR algorithm we have designed allocates different roles to the IMMU sensors. The gyro is given the task to provide short-term accurate a priori estimates of the state vector, in particular the rotation quaternion. During each EKF run, the acceleration measurements taken from a swinging leg are in fact prevented from influencing the filter behavior by properly applying the measurement validation test (18); meanwhile, the measurement validation test (18) tends to increase the measurement noise variance of the magnetic sensor when it is exposed to external magnetic disturbances over the value prescribed in a magnetically clean environment, so that, when the a posteriori estimate of the vector state has to be formed, the EKF tends to put more confidence on the a priori estimate than on the actual sensor measurements. Since the tri-axis gyro in our shoe-mounted IMMU is thermally compensated, it is sufficient to capture the bias offset at the start of the experimental session to have a well-calibrated sensor for several minutes before the next bias capture, which can be performed anytime the tri-axis gyro is detected to be motionless. In our approach, the effects of random walk errors due to gyro wideband noise integration are counteracted by letting the EKF to run over single movement epochs, i.e., single strides in the case of normal gait. We remind that, in Method A, the g-rejections tend to increase the duration of the EKF run, and to delay the application of the TRIAD algorithm until quasi-static gravity read-outs are available. The magnetic measurements are bias-compensated for use by the iterated-TRIAD algorithm, depending on whether an h-rejection occurs at the time of alignment or not; conversely, the zero velocity updates are applied to gravity-compensated linear accelerations as frequently as possible.

The results of the outdoor walking trial indicate that positioning errors are less than 0.6% for both Method A and B, with a slight preference for Method A. Of course, this conclusion would be taken with care, because the truth-reference is, on its own, affected by errors (RMS of about 5 m are declared by the manufacturer). However, it is interesting that a relatively low-cost GPS unit shows similar levels of accuracy of a simple IMMU when a) the GPS works in nearly optimal conditions b) the IMMU works over a temporal

horizon for which, it is quoted, would be very difficult to keep the error growth small (Foxlin, 2002).

It is interesting to note that the outdoor walking trial is traveled over an asphalt road, whose incline (in the direction of movement) is approximately constant. After few strides taken on a level surface, the path is traveled, first downhill, up to the time of turning around, and then uphill. That the first strides are taken on a level surface, it is important, because the first step of our computational procedure is to register the sensor frame to the reference frame. First, the unit is calibrated; second, the unit is placed on the level walking surface, and the expression of the referential magnetic field is estimated from the calibrated magnetic sensor measurements.

Because of the axis arrangement, the difference in the roll angle estimated uphill and downhill would give an indication of the slope of the walking surface. An estimation of the same quantity comes from taking the horizontal and vertical displacements. Since the agreement between these two estimates turns out to be quite good, we can speculate that the foot posture at the time of alignment is estimated reasonably well in terms of roll and pitch angles. By closer examination of the filtering results, it is the foot yaw angle estimate to be critical, which may lead to catastrophic results especially when the gyro integration is left free running.

In conclusion, an adaptive quaternion-based EKF algorithm is developed in this paper to process the sensory data from a fully integrated IMMU, deployed in a shoe-mounted PNS. The traveled path is then reconstructed by stride-wise strap-down double integration of foot accelerations resolved in the navigation frame. In order to make the filtering process robust against the disturbances which may affect the IMMU sensors , several tricks are considered:

- adaptation of the measurement noise covariance matrix during EKF runs;
- adaptive alternation between initialization and run of the EKF, so as to refine the estimation of either the rotation quaternion or the magnetic sensor bias vector – this is based on stance/swing phase gait detection driven by gyroscopic data, and accelerometric/magnetic measurement validation;
- bias-correction of the magnetic sensor measurements before using them for initializing each EKF run;
- stride-wise integration of gravity-compensated acceleration components with zero velocity updates performed once every movement epoch is detected.

Preliminary experimental results are offered in support of the use of inertial/magnetic sensing and EKF for implementing dead-reckoning algorithms in applications of personal navigation.

6. Acknowledgement

This work has been supported, in part, by funds from the Italian Ministry of University and Research. The author is indebted to Dr. Vincenzo Genovese, for his help in programming the PC sensor interface used for data collection.

7. References

Elwell J. (1999). Inertial navigation for the urban warrior. *Proceedings SPIE,* vol. 3709, pp. 196-204, Orlando, FL, USA, 7-8 April 1999.

Fang L.; Antsaklis, P.J., Montestruque, L.A., McMickell, B., Lemmon, M., Sun, Y., Fang H., Koutroulis, I., Haenggi, M., Xie, M. & Xie, X. (2005). Design of a wireless assisted pedestrian dead reckoning system – The NavMote experience. *IEEE Trans. Instrum. Meas.*, Vol. 54, No. 6, pp. 2342-2358.

Foxlin, E. (2002). Motion tracking requirements and technologies, In: *Handbook of virtual environment technologies*, K. Stanney, (Ed.), pp. 163-210, Lawrence Erlbaum Publishers, Hillsdale, NJ, USA.

Gebre-Egziabher D.; Elkaim G.H., Powell J.D. & Parkinson B.W. (2000). A gyro-free quaternion-based attitude determination system suitable for implementation using low cost sensors. *Proc. IEEE Position, Location and Navigation Symposium*, pp. 185-192, San Diego, CA, USA, 13-16 March, 2000.

Jirawimut, R.; Ptasinski, P., Garaj, V., Cecelja, F. & Balachandran, W. (2003). A method for dead reckoning parameter correction in pedestrian navigation system. *IEEE Trans. Instrum. Meas.*, Vol. 52, No. 1, pp. 209-215.

Ladetto, Q. & Merminod B. (2002). In step with INS – navigation for the blind, tracking emergency crews. *GPS World*, October 2002, pp. 30-38.

Lee, S.-W. & Mase K. (2002). Activity and location recognition using wearable sensors. *Pervasive Computing*, Vol. 1, No. 1, pp. 24-32.

Perrin O.; Terrier, P., Ladetto, Q., Merminod, B. & Schutz, Y. (2000). Improvement of walking speed prediction by accelerometry and altimetry, validated by satellite positioning. *Med. Biol. Eng. Comput.*, Vol. 38, No. 2, pp. 164—168.

Sabatini, A.M. (2005). Quaternion based strap-down integration method for applications of inertial sensing to gait analysis. *Med. Biol. Eng. Comp.,* Vol. 43, No. 1, pp. 94-101.

Sabatini, A.M.; Martelloni, C., Scapellato, S., & Cavallo, F. (2005). Assessment of walking features from foot inertial sensing. *IEEE Trans. Biomed. Eng.*, Vol. 52, No. 3, pp. 486-494.

Sabatini, A.M. (2006). Quaternion based Extended Kalman filter for determining orientation by inertial and magnetic sensing. *IEEE Trans. Biomed. Eng.*, Vol. 53, No. 7, pp. 1346-1356.

Shuster, M.D. & Oh S.D. (1981). Three-axis attitude determination from vector observations. *J. Guidance and Control*, Vol. 4, No. 1, pp. 70-77.

Stirling, R.; Fyfe, K. & Lachapelle, G. (2005). Evaluation of a new method of heading estimation for pedestrian dead reckoning using shoe mounted sensors. *Journal of Navigation*, Vol. 58, No. 1, pp. 31-45.

Veltink, P.H.; Slycke, P. , Hemssems, J., Buschman, R., Bulstra, G. & Hermens, H. (2003). Three dimensional inertial sensing of foot movements for automatic tuning of a two-channel implantable drop-foot stimulator. *Med. Eng. Phys.*, Vol. 25, No. 1, pp. 21—28.

Welch, G. & Foxlin E. (2002). Motion tracking: no silver bullet, but a respectable arsenal. *IEEE Computer Graphics and Applications*, Vol. 22, No. 6, pp. 24-38.

Yun, X. & Bachmann, E.R. (2006). Design, implementation, and experimental results of a quaternion-based Kalman filter for human body motion tracking. *IEEE Trans. Robotics*, Vol. 22, No. 6, pp. 1216–1227.

Kalman Filter Recent Advances and Applications

Edited by Victor M. Moreno and Alberto Pigazo

ISBN 978-953-307-000-1
Hard cover, 584 pages
Publisher InTech
Published online 01, April, 2009
Published in print edition April, 2009

The aim of this book is to provide an overview of recent developments in Kalman filter theory and their applications in engineering and scientific fields. The book is divided into 24 chapters and organized in five blocks corresponding to recent advances in Kalman filtering theory, applications in medical and biological sciences, tracking and positioning systems, electrical engineering and, finally, industrial processes and communication networks.

InTech Europe
University Campus STeP Ri
Slavka Krautzeka 83/A
51000 Rijeka, Croatia
Phone: +385 (51) 770 447
Fax: +385 (51) 686 166
www.intechopen.com

InTech China
Unit 405, Office Block, Hotel Equatorial Shanghai
No.65, Yan An Road (West), Shanghai, 200040, China
中国上海市延安西路65号上海国际贵都大饭店办公楼405单元
Phone: +86-21-62489820
Fax: +86-21-62489821

IntechOpen